PROCEEDINGS OF SCIENCE

Digital methods of RFI mitigation in radio astronomy

M. K. Lebedev,* **N. E. Ovchinnikova, V. M. Bogod, A. M. Ripak and A. A. Storozhenko**

Special Astrophysical Observatory of RAS,
Nizhny Arkhyz, Russia
E-mail: m.k.lebedev@gmail.com, n.e.ovchinnikova@gmail.com, vbog_spb@mail.ru, anatoly.ripak@gmail.com, acs-work@mail.ru

We describe a new spectropolarimetric receiving complex for solar observations with the RATAN-600 radio telescope in the decimeter wavelength range. The use of a high-speed ADC and FPGA-based design of the DSP section made possible the direct detectorless reception and processing of radio frequency signals. The complex makes use of a method of radio frequency interference (RFI) mitigation based on the statistical properties of the received noise signal. We provide a brief description of the method, as well as details of the receiving system design, and give an example of the handling of data obtained from solar observations.

The Multifaceted Universe: Theory and Observations - 2022 (MUTO2022)
23-27 May 2022
SAO RAS, Nizhny Arkhyz, Russia

*Speaker

PoS(MUTO2022)006

Introduction

The design frequency range of the RATAN-600 radio telescope spreads over the part of the radio spectrum from 0.6 to 37.5 GHz (50–0.8 cm). During the last decades, its site has experienced drastic deterioration of the interference environment. The most severe radio frequency interference (RFI) occurs in the low-frequency part of the instrument's range. For this reason, observations at frequencies lower than 3 GHz were stopped in the mid-2010s. Nonetheless, there are plenty of phenomena, especially in solar physics, which manifest themselves just in the 0.5–3 GHz band, thus it would be very desirable to resume the observations in that frequency range.

The RATAN-600 has accumulated a wealth of experience in dealing with RFI. As the interference environment changed over time, methods of RFI mitigation changed as well. While during the 1980s and in the beginning of the 1990s, most RFI were short-time noise surges, which could be successfully suppressed by time selection based on discrimination of signal values exceeding a certain threshold [1], in the next years the development of wireless communications, satellite television systems, microwave ovens, etc. resulted in long-lasting RFI, which took more sophisticated methods for their excision and suppression acting in both time and frequency domains [2]. Signal from the quadratic detector of the radiometer was digitized in the band up to 32 kHz wide, and the number of the radiometer outputs was 4–8 rather than one, as in earlier designs, dividing the radiometer frequency band into several narrow channels using the analog band-pass MW filter bank. This allowed for digital pulse interference suppression in every narrow channel, as well as the selection of channels free from RFI that could not be suppressed using those methods. The RFI mitigation techniques based on this principle have been used on the RATAN-600 up to the present time. However, as the selection of narrow channels from the full bandwidth is done by means of analog filtering, any system of this type has a natural limitation both on the number of frequency channels (i. e. on the frequency resolution) and on the overall bandwidth. The systems of RFI suppression were implemented for relatively narrow wavelength ranges around 13 cm, 31 cm, and 49 cm. A device of this kind with a frequency range of one octave or more seems to be impractical.

The advent of gigasample ADCs and recent progress in DSP techniques using fast processing algorithms implemented in FPGAs have made possible the development of detectorless receiving systems that perform the direct analog to digital conversion of RF signals and their further on-the-fly processing. The relative bandwidth of such a system can be very large, and the achievable frequency resolution is limited only by the number of points in discrete Fourier transform, which can easily be made as high as 2^{10}–2^{16}, depending on the size and number of used FPGAs. Unlike previous generations of instruments, these digital systems can be made *dynamic*, in that the suppressed regions of the time-frequency domain may vary depending on the RFI situation at the particular moment. Note that the most powerful interference, such as cell phone and other wireless communication signals, still may require to be filtered out by means of analog filtration in order to prevent intermodulation distortions or even saturation of input amplifiers. Moreover, in the case of the RATAN-600 site, RFI spectral distribution and power density in the frequency range below 1 GHz render impossible any radio astronomical observations, except perhaps for a few separate narrow spectral bands.

1. Statistical methods of RFI excision

Methods of RFI excision exploiting the analysis of statistical properties of the spectra of received noise signals are based on the assumption that astrophysical signals of natural origin have Gaussian statistics, while non-Gaussian artificial interference would introduce certain distortion into the statistical properties of the signal.

Consider some Gaussian "useful" signal with zero mean. The noise of the receiving system is Gaussian and has zero mean as well. Real and imaginary parts of the discrete Fourier spectrum components of such a signal are themselves statistically independent Gaussian processes with zero mean. Instantaneous power spectrum is a sum of squares of real and imaginary parts of the discrete Fourier spectrum, thus each of its components except for the DC and Nyquist frequency has χ^2 statistics with two degrees of freedom. The relative statistical fluctuation of the power spectrum density (PSD) in the k-th frequency bin can be characterized [3] by a dimensionless magnitude

$$V_k^2 = \frac{\sigma_k^2}{\mu_k^2}, \tag{1}$$

where μ_k and σ_k are mean and standard deviation of PSD in this bin:

$$\mu_k = \langle P_k \rangle ; \qquad \sigma_k = \left\langle P_k^2 \right\rangle - \langle P_k \rangle^2 ;$$

P_k is a PSD estimate. V_k^2 is referred to as spectral variability. It can be shown that for a Gaussian signal

$$\begin{aligned} V_k^2 &= 2 \qquad \text{if } k = 0 \text{ or } k = N/2; \\ V_k^2 &= 1 \qquad \text{otherwise,} \end{aligned}$$

where N is a DFT length, hence $N/2$ is a number of the frequency bin corresponding to the Nyquist frequency, and $k = 0$ corresponding to the DC component. Special values of V_k^2 at these frequencies arise from the fact that, unlike the other ones, these components are pure real, and their probability distribution is χ^2 with *one* degree of freedom.

Furthermore, one can show [4] that (1) is equivalent up to a constant to

$$K(f_k) = \frac{\left\langle A_k^4 \right\rangle}{\left\langle A_k^2 \right\rangle^2}, \tag{2}$$

where A_k is either a real or imaginary part of the DFT component in a k-th frequency bin. Equation (2) is a definition of a *kurtosis*, that is a normalized fourth central moment of the probability distribution of A_k. $K(f_k)$ is expected to be exactly 3 for a Gaussian process.

In [5] the following estimator for the *spectral kurtosis* was proposed:

$$\hat{V}_k^2 = \frac{\hat{\sigma}_k^2}{\hat{\mu}_k^2},$$

where $\hat{\sigma}_k^2$ and $\hat{\mu}_k$ are unbiased estimators of their associated parameters σ_k^2 and μ_k. Introducing notations

$$S_1 = \sum_{i=1}^{M} P_{ki}, \qquad S_2 = \sum_{i=1}^{M} P_{ki}^2,$$

one can show that

$$\hat{V}_k^2 = \frac{M}{M-1}\left(M\frac{S_2}{S_1^2} - 1\right),$$

which is expected to be 1 for a Gaussian process.

At this point, we have a recipe which allows us to discriminate between a "useful" Gaussian signal and a signal contaminated with a non-Gaussian interference: (a) take $N \times M$ time samples; (b) for each N samples calculate the DFT; (c) calculate the absolute squares of M obtained spectra, i. e. PSDs; (d) for each spectral component calculate the estimator $\hat{V}_k^2$; (e) if the difference between the estimate obtained and 1 is outside of a certain predefined range, then tag the corresponding value as contaminated with RFI; (f) otherwise, pass the S_1 value, considering it as a "good" one.

It is vital for the hardware implementation of this recipe that the DFT and accumulation of S_1 and S_2 can be done in a pipelined manner, thus providing stream processing of the input data.

The described method has been successfully applied for RFI excision on the EOVSA FASR Subsystem Testbed facility, Korean Solar Radio Burst Locator, and some other radio telescopes.

2. Digital spectropolarimetric complex with RFI excision for solar observations with the RATAN-600

In order to resume solar observations in the decimeter wavelength range with the RATAN-600 it was decided to develop a new spectropolarimetric receiving complex with RFI excision based on the spectral kurtosis method. The design goals were set as follows: frequency range: 1–3 GHz, frequency resolution: 0.12–10 MHz, time resolution: ~10 ms, dynamic range: > 60 dB. We describe below the result of this development effort.

2.1 Analog frontend

The block diagram of the analog part of the receiving complex is shown in Fig. 1. There are two separate channels for left and right circular polarizations, each containing its own low noise amplifier (LNA) with a gain of 17-20 dB over the passband. The polarization channels work alternately, being selected by a switch controlled by a host computer. The amplified signal passes three band-stop filters that suppress the most contaminated frequency bands, and low-pass and high-pass filters, which perform preliminary shaping of the device's passband. After further amplification by another two LNAs, the signal is divided equally between two channels with the passbands 1–2 GHz and 2–3 GHz respectively, each containing a host controlled step tunable 0–30 dB attenuator and a high-gain amplifier. Together with a similar attenuator in the common part of the signal path, this arrangement provides semi-independent gain control in the 60 dB range for either frequency channel. Thorough gain monitoring and control are necessary in order to prevent the overload of the amplifiers, as once the system exits linear mode, the intermodulation interference over the whole spectrum arises, which cannot be eliminated by digital processing. A power meter and a socket for test purposes are coupled to the output path of each frequency channel. The antenna inputs may be switched off, connecting to the noise generator for system calibration instead.

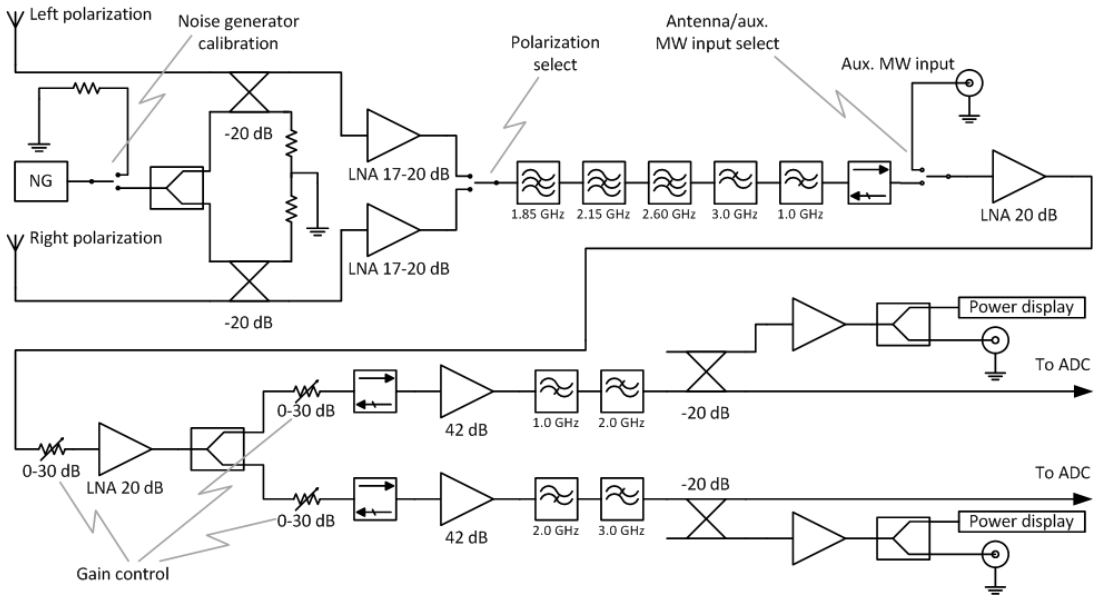

Figure 1: Analog frontend of the receiving complex

2.1.1 Digital data processing section

The digital data processing section is built on the Xilinx VC707 evaluation board with the 4DSP fmc126 mezzanine ADC board. The ev10aq190a 10 bit ADC is used to digitize the input analog signal at 2 GSPS in two frequency channels, 1–2 GHz and 2–3 GHz respectively, thus operating in undersampling mode. It is clocked by the signal from a 2 GHz stabilized quartz generator. Data processing itself is performed in Virtex-7 FPGA, which is linked with the ADC via LVDS interface. There are two identical data processing pipelines for two frequency channels. The output data are sent to the host computer over 1G Ethernet. The Microblaze CPU implemented in FPGA fabric is used for the system setup and control of the peripheral equipment. The block diagram of the digital section and the signal flow are shown in Fig. 2.

Fig. 3 shows the data processing pipeline in more detail. The ADC in two-channel mode presents two samples on its output in every clock cycle for either channel. The deserializers decrease the clock rate of the data stream by a factor of 8, yielding 16 samples in each clock cycle. Demultiplexer combines and rearranges the data, dividing it into eight data streams. Each stream then undergoes the 2048-point FFT, and the resulting values are multiplied by $\exp[-i2\pi jk/(MN)]$, where j is the channel number, k is the point number in the current channel, $M = 8$ is the number of channels, $N = 2048$ is the number of points in each FFT. The 8-point FFT performs the last stage of the long 16384-point transform. Because the input signal is real, only 8192 points are used in further calculations. Next downstream is a block that computes and accumulates P_i and P_i^2 values over each of the 1024 successive spectra, calculates the spectral kurtosis estimator and tags data with the obtained values. The multiplexer rearranges the data, combining eight streams into one. At this point, the data stream is reduced by a factor of 2×1024. The output stream shaper performs the averaging over adjacent frequency channels, depending on the required frequency resolution, and outputs the result, as well as the percentage of "good" values contributed to the particular point,

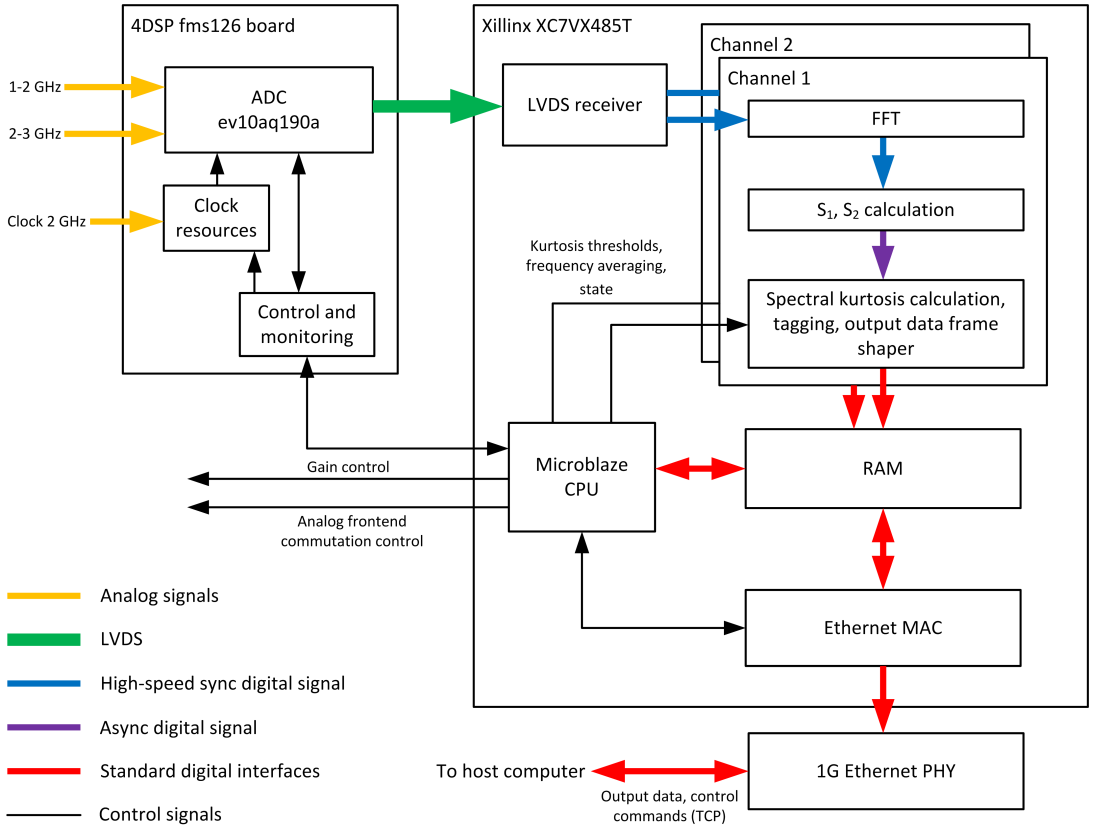

Figure 2: Signal flow in digital backend

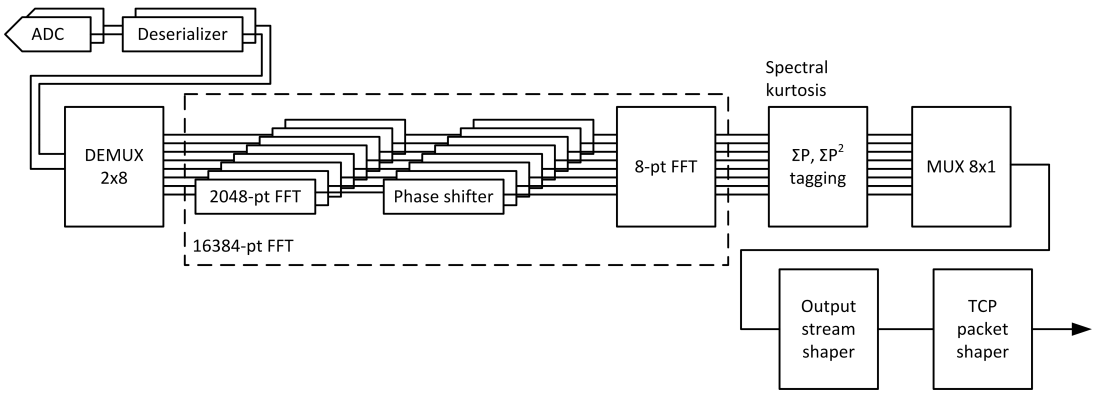

Figure 3: Digital data processing pipeline

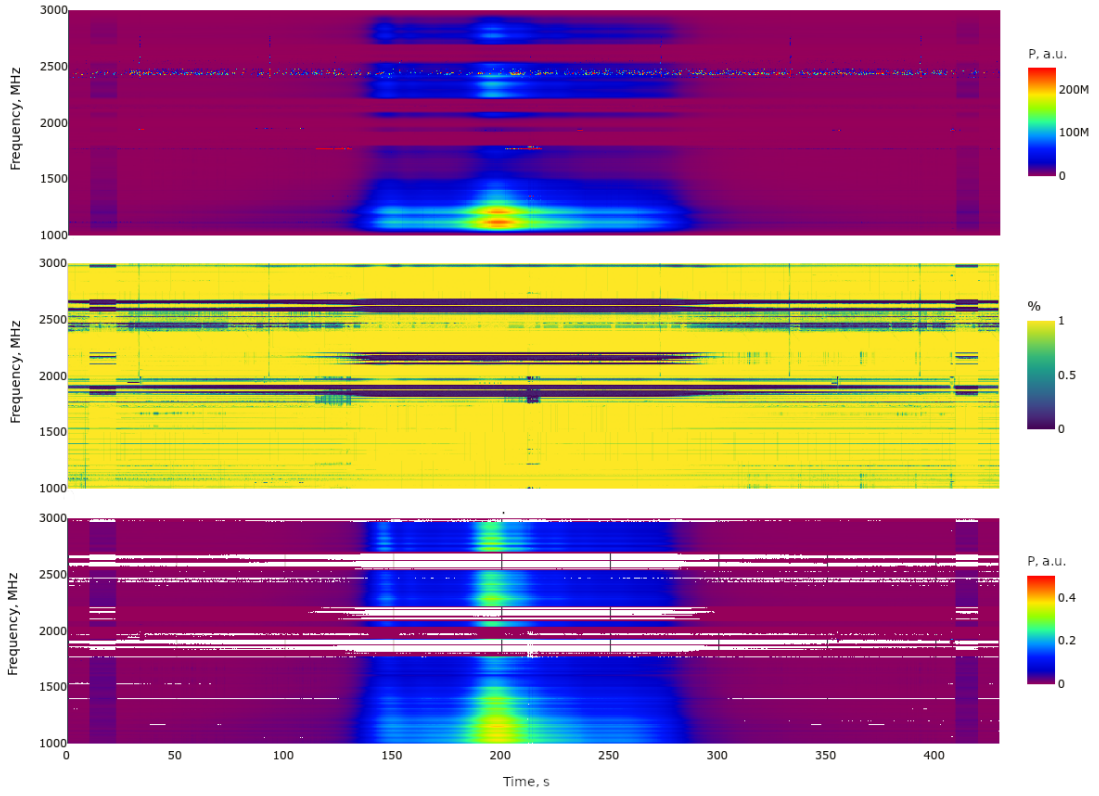

Figure 4: 2022-03-27 solar observation. *Top:* raw data; *center:* percentage of "good" values; *bottom:* data after cleaning and calibration

which is a measure of confidence of the given value. The TCP packet shaper splits the data stream into portions suitable to be wrapped into network packets.

2.2 Characteristics of the complex

The receiving complex has the following technical parameters: frequency range 1–3 GHz; full frequency resolution 122.070 kHz; output frequency resolution 488–7812 KHz; time resolution: 8.4 ms; dynamic range 90 dB (that is dynamic range of the digital system of 30 dB plus analog attenuation 0–60 dB).

To date, a few series of radio astronomical observations have been carried out. Based on their results, the following conclusions have been made about the real characteristics of the receiving complex. The equivalent noise temperature of the receiver is in the range 45–100 K, depending on frequency. The equivalent noise temperature of the receiving system, including the antenna, is 200–350 K in the entire range of 1–3 GHz. In the situation when RFI is weak, the sensitivity of the receiver is close to its theoretical value if the averaging time $t_a \lesssim 1$ s, and decreases as t_a gets longer due to flicker noise. Strong RFI, even if it can be excised by analog filters and statistical cleaning, leads to a 4–10-fold degradation of the sensitivity in comparison with the theoretical value at frequencies up to 2700 MHz, while at higher frequencies there are at least several intervals where the sensitivity is close to the theoretical value.

2.3 Solar observations example

In Fig. 4 an example of data from solar observations is presented. The observation was performed on 2022.03.27 around 09:00 UTC (RATAN-600 +4th azimuth). The top panel shows the raw data in the form of a spectrogram, as it was obtained from the receiving complex. The middle panel depicts the corresponding time-frequency distribution of the percentage of "good" data values involved in the calculation (averaging over frequency bands) of output data points. This distribution serves as a mask, which is applied to the raw data in order to eliminate data points where the signal had mostly non-Gaussian statistics, hence believed to be contaminated with RFI. In the bottom panel, the result of this masking and subsequent calibration is given. For the detailed description of the calibration procedure and further observation data processing, see our paper "Results of the new approach to the analysis of multi-wavelength observations data on RATAN-600" in the current Proceedings.

3. Conclusion

The receiving complex we have created allows us to resume the solar observations with the RATAN-600 radio telescope in the decimeter range. It has much better time and frequency resolution compared to the previous generations of equipment, which had been used until the deterioration of the RFI environment made observations impossible. With the RFI mitigation method used, the observations can be carried out in ~75% of the 1–3 GHz frequency range.

Acknowledgments

Observations with the SAO RAS telescopes are supported by the Ministry of Science and Higher Education of the Russian Federation. The renovation of telescope equipment is currently provided within the national project "Science and Universities". The work was performed as part of the SAO RAS government contract approved by the Ministry of Science and Higher Education of the Russian Federation.

References

[1] A. A. Gorbachev, V. I. Danilov, Yu. I. Modeev, *Device for the processing of noise signals against the background of interference in a modulation radiometer,* Instr. and Exp. Techn. **4** (1987) 83.

[2] P. G. Tsybulev, A. B. Berlin, N. A. Nizhel'skij et al., *Interference-mitigation measures at RATAN-600 radio telescope,* Astrophys. Bull. **62** (2007) 193.

[3] J. Kenney, E. Keeping, *Mathematics of Statistics*, D. Van Nostrand Company, Princeton 1962.

[4] R. Dwyer, *Detection of non-Gaussian signals by frequency domain Kurtosis estimation,* in proceedings of *ICASSP '83. IEEE International Conference on Acoustics, Speech, and Signal Processing*, IEEE, Boston, MA 1983.

[5] G. M. Nita, D. E. Gary, Zhiwei Liu et al., *Radio frequency interference excision using spectral-domain statistics,* PASP **119** (2007) 805.